



Published in final edited form as:

*Chembiochem*. 2009 August 17; 10(12): 1959–1964. doi:10.1002/cbic.200900172.

## Disruption of Transcriptionally Active Stat3 Dimers with Non-phosphorylated, Salicylic Acid-Based Small Molecules: Potent *in vitro* and Tumor Cell Activities

Steven Fletcher<sup>[a]</sup>, Jagdeep Singh<sup>[a]</sup>, Xiaolei Zhang<sup>[b]</sup>, Peibin Yue<sup>[b]</sup>, Brent D. G. Page<sup>[a]</sup>, Sumaiya Sharmeen<sup>[c]</sup>, Vijay M. Shahani<sup>[a]</sup>, Wei Zhao<sup>[b]</sup>, Aaron D. Schimmer<sup>[c]</sup>, James Turkson<sup>[b]</sup>, and Patrick T. Gunning<sup>[a]</sup>

Patrick T. Gunning: patrick.gunning@utoronto.ca

<sup>[a]</sup> Department of Chemistry, University of Toronto, Mississauga Mississauga, ON L5L 1C6 (Canada) Fax: (+1) 905-828-5425

<sup>[b]</sup> Department of Molecular Biology and Microbiology Burnett College of Biomedical Sciences, University of Central Florida Orlando, FL 32826 (USA) Fax: (+1) 407-384-2062

<sup>[c]</sup> Ontario Cancer Institute/Princess Margaret Hospital 610 University Avenue, Toronto, ON M5G 2M9 (Canada) Fax: (+1) 416-946-6546

### Keywords

antitumor agents; molecular recognition; molecular therapeutics; protein-protein interactions; stat3

Signal transducer and activator of transcription 3 (Stat3) protein is a cytosolic transcription factor that relays signals from receptors in the plasma membrane directly to the nucleus, and is routinely hyperactivated in many human cancers and diseases.[1] Regarded as an oncogene, Stat3 is well-recognized as a master regulator of cellular events that lead to the cancer phenotype, making this protein viable target for molecular therapeutic design.[2] Stat3 inhibitors have included peptides,[3–4] peptidomimetics,[5–9] small molecules[10–14] and metal complexes.[15] Despite significant advances in Stat3 inhibition,[1] truly potent (*in vivo*), isoform-selective, small molecule Stat3 agents have not been readily forthcoming; this is likely due in part to the challenge of disrupting protein–protein interactions.[16]

The canonical view of Stat3 signaling describes inactive Stat3 monomers located predominantly within the cytoplasm. The Stat3 activation pathway begins with a cytokine or growth factor ligand interaction with the extracellular domain of a transmembrane receptor. Subsequently, receptor-associated tyrosine kinases such as the Janus kinases (Jaks) are induced to phosphorylate tyrosine residues on the specific receptor's cytoplasmic domain. These phosphorylated residues then serve to recruit latent Stat monomers through interaction with their SH2 domains. Tyrosine-kinase-mediated phosphorylation of Tyr705 on Stat3 monomers induces Stat3–receptor dissociation and Stat3–Stat3 homodimerization through reciprocal phosphotyrosine (pTyr)–SH2 domain interactions. The resulting transcriptionally active Stat3 dimers then translocate to the nucleus, where they bind to specific DNA-response elements in the promoters of target genes and induce antiapoptotic gene expression programs (e.g., Bcl-x<sub>L</sub>) and the overexpression of cell cycle regulators (for example, cyclin D<sub>1</sub>).[17] Current programs of research, including our own, have focused on inhibiting the

dimeric protein complex as a route to suppressing Stat3 transcriptional profiles. Disruption of Stat3–Stat3 protein–protein interactions has been achieved through SH2 domain binders that effectively compete with phosphorylated Stat3 monomers for the pTyr-binding module. [1a,d]

Our research groups have previously identified the potent, cellular Stat3 inhibitor **S3I-201** (Figure 1A;  $IC_{50} = 86 \mu\text{M}$ ) through in silico structure-based virtual screening of National Cancer Institute chemical libraries.[12] We sought to optimize lead agent **S3I-201** through rational, synthetic modifications with the global objective of obtaining isoform-selective, Stat3 inhibitors displaying potency at low to submicromolar concentrations. **S3I-201** is based on a glycolic acid scaffold whose carboxylic acid functionality has been condensed with 4-aminosalicylic acid to furnish the amide bond, and whose hydroxyl has been tosylated (Figure 1A). The Stat3 SH2 domain is broadly composed of three subpockets, but GOLD[18] docking studies showed that **S3I-201** can access only two of these subpockets simultaneously (Figure 1B), and this identified a potential means of improving inhibitor potency. The salicylic (*ortho*-hydroxybenzoic) acid component of **S3I-201** is a known pTyr mimetic,[20] and low-energy GOLD docking studies consistently placed this unit in the pTyr-binding site, where it makes hydrogen bonds and salt bridges with Lys591, Ser611, Ser613 and Arg609. Due to the strength of interactions between oppositely charged ions, here the anionic carboxylate of **S3I-201** and the cationic side-chains of Lys591 and Arg609, it is likely that a considerable portion of the binding energy between the SH2 domain and **S3I-201** arises from the pTyr mimetic. The *O*-tosyl group binds in the mostly hydrophobic pocket that is derived from the tetramethylene portion of the side-chain of Lys592 and the trimethylene portion of the side-chain of Arg595, along with Ile597 and Ile634. Given the moderate potency of **S3I-201** towards Stat3 inhibition and the previously mentioned opportunity for increasing SH2 domain interactions, a rational synthetic program was undertaken to modify and optimize this small molecule to furnish more potent analogues.

**S3I-201** contains the excellent tosylate leaving group, which is especially susceptible to nucleophilic attack in this case due to its positioning  $\alpha$  to a carbonyl group. Therefore, although we have no conclusive proof that **S3I-201** operates as an irreversible inhibitor, there are several nucleophilic residues on the Stat3 SH2 domain surface, such as Cys712 and Cys418, and the potential alkylating ability of **S3I-201** might thwart a structure–activity relationship study. Thus, we decided to replace the scaffold oxygen of the tosylate group with a nitrogen atom to render the tosyl group no longer labile. Since GOLD docking studies consistently placed the resulting tosylamide moiety in the same Ile597/Ile634 hydrophobic subpocket as the tosylate in **S3I-201**, completing the valency of this nitrogen with a hydrogen atom was anticipated to be detrimental to inhibitor binding because this would afford a polar NH group. Hence, we were especially keen to replace the oxygen atom with the more hydrophobic NCH<sub>3</sub> and NBoc groups. Another region of the lead molecule that we wanted to modify was the NH of the amide bond, which provides an ideal platform from which to further functionalize **S3I-201** and thereby gain access to the third, as-yet-unexplored hydrophobic subpocket (Trp623, Val637, Ile659 and Phe716) of the SH2 domain (Figure 1B, yellow arrow). Moreover, alkylation of this NH group would furnish a more hydrophobic tertiary amide functionality, which, according to GOLD docking studies, would be expected to enhance inhibitor binding. Thus, we initially had two goals. First, we wanted to substitute the scaffold oxygen with alternative hydrophobic groups that would destroy the alkylating potential of the tosylate group. Second, we wanted to functionalize the NH of the amide group of **S3I-201** with hydrophobic moieties to achieve improved inhibitor affinity for the Stat3 SH2 domain by making van der Waals' contacts with the third subpocket of the domain.

To these ends, we modified **S3I-201** as shown in Table 1. For inhibitors where X = NCH<sub>3</sub>, the synthetic route followed is depicted in Scheme 1; similar series of transformations were executed for the remaining inhibitors (X=O, NH and NBoc), and these syntheses are given in full in the Supporting Information. The carboxylic acid and hydroxyl functional groups of 4-amino-salicylic acid (**1**) were stepwise protected in one pot as their benzyl ester and ether, respectively, by two rounds of treatment with benzyl bromide (BnBr) and potassium *tert*-butoxide (KO*t*Bu) as base to furnish aniline **2**. Subsequently, a variety of hydrophobic aldehydes (RCHO) were reductively aminated with **2** in very good to excellent yields, affording the corresponding series of secondary anilines **3**. Meanwhile, in this convergent synthetic strategy, the sulfonamide portion of the target molecules was prepared in parallel. Specifically, glycine methyl ester (**4**) was treated with *p*-tosyl chloride (*p*-TsCl) and then the nitrogen atom of resultant sulfonamide **5** was methylated with methyl iodide (MeI) to give **6**. Lithium hydroxide readily effected methyl ester hydrolysis to furnish the free acid **7** in an overall yield of 75 % (three steps).

Condensation of the series of anilines **3** with acid **7** was accomplished with the peptide coupling agent dichlorotriphenylphosphorane (PPh<sub>3</sub>Cl<sub>2</sub>) to give tertiary amides **8** in very good to excellent yields. Finally, a global debenylation with hydrogen gas and palladium on carbon (10 % Pd/C) as catalyst delivered the **S3I-201** analogues **9**. It is noteworthy that compounds containing aryl nitrile moieties were chemoselectively debenzylated under these conditions, with only trace amounts of reduced nitrile byproducts observed. These observations are likely due to a combination of fast reaction times (both aryl nitrile-containing compounds were doubly debenzylated in about 1 h), which limited the exposure of the nitrile to the reductive conditions, and the fortuitous limited solubilities of compound **8** in neat MeOH, requiring the use of the cosolvent THF, which is known to suppress hydrogenation of nitriles.[21] On the other hand, for the deprotection of the precursor to inhibitor **SF-1-085** (Table 1), which incorporates an aryl–bromide bond, hydrogenolysis was not deemed a practical procedure, given that reduction of aryl–halide bonds with hydrogen gas and Pd/C is a relatively facile side reaction.[22] Instead, we adopted a high-yielding, nonreductive, two-step method that involved the selective hydrolysis of the benzyl ester with LiOH, followed by our previously reported TFA-mediated debenylation of the aryl benzyl ether.[23]

Inhibition of Stat3 dimerization *in vitro* was judged by the abilities of the small molecules to disrupt Stat3–Stat3:DNA-binding activity by conducting an electrophoretic mobility shift assay (EMSA; Figure 2), performed as described previously.[3] IC<sub>50</sub> values were obtained by quantifying residual DNA-binding activities by using ImageQuant.[3] A companion paper by Zhang et al. describes in detail the biochemical and biological evaluations of **SF-1-066** (also known as **S3I-201.1066**).[24] As shown in Table 1, initial synthetic modulations to the **S3I-201** heteroatom X group were unsuccessful. In fact, negligible activity (IC<sub>50</sub> > 300 μM) was observed for X = NH (**SF-1-082**) X = NCH<sub>3</sub> (**SF-1-071**) and X = NBoc (**SF-1-091**, Figure 2A) analogues of lead inhibitor **S3I-201**. The drop in activity observed upon modification of the labile *O*-tosyl functionality to the non-labile *N*-tosyl functionalities lends support that **S3I-201** might operate, at least in part, as an irreversible inhibitor by alkylating the Stat3 SH2 domain. Nevertheless, upon replacement of R<sup>1</sup> = H (**SF-1-071**) with R<sup>1</sup> = Bn (**SF-1-062**), some recovery in inhibitor potency (IC<sub>50</sub> = 292 μM) was observed, which, with X = NCH<sub>3</sub> in both cases, can no longer be ascribed to irreversible inhibition and is likely due to enhanced noncovalent interactions with the target protein surface.

Encouraged by these findings, we proceeded with constructing a series of simple *meta* and *para*-substituted *N*-benzyl derivatives of **S3I-201** in which X was fixed as NCH<sub>3</sub>. Replacement of the R<sup>1</sup> benzyl group in **SF-1-062** with *para*-cyanobenzyl (**SF-1-073**) led to

an improvement in activity ( $IC_{50} = 260 \mu\text{M}$  for **SF-1-073**, as compared to  $IC_{50} = 292 \mu\text{M}$  for **SF-1-062**). This enhancement in Stat3 inhibition might be due either to improved hydrophobic interactions with the larger and more electron poor, aromatic system, or from a hydrogen bond between the nitrile group and an SH2 domain backbone NH. More interesting is the observation that Stat3 inhibition improved with the increasing size of hydrophobic  $R^1$  group. Specifically, *para*-(*tert*-butyl)benzylated agent **SF-1-068** showed marked improvement in activity over both **SF-1-062** ( $R^1 = \text{benzyl}$ ) and **SF-1-073** ( $R^1 = \textit{para}$ -cyanobenzyl). Furthermore, **SF-1-070** ( $R^1 = \textit{para}$ -(phenyl)benzyl), which incorporates a large biphenyl moiety, displayed an almost twofold increase in potency compared to the smaller *para*(*tert*-butyl)benzyl derivative (**SF-1-070**:  $IC_{50} = 115 \mu\text{M}$  cf. **SF-1-068**:  $IC_{50} = 194 \mu\text{M}$ ). The inclusion of the especially hydrophobic (*para*-cyclohexyl)benzyl group in the  $R^1$  position furnished an inhibitor that exhibited Stat3 inhibitory activity with more than double the potency of our lead agent:  $IC_{50} = 35 \mu\text{M}$  for **SF-1-066** (Figure 2B; cf.  $IC_{50} = 86 \mu\text{M}$  for **S3I-201**). Moreover, in nuclear extracts containing activated Stat1, Stat3 and Stat5 prepared from EGF-stimulated NIH3T3/hEGFR (mouse fibroblasts overexpressing the human epidermal growth factor receptor, EGF), **SF-1-066** was shown to display promising Stat3 isoform selectivity, preferentially inhibiting Stat3 complexes over both Stat1 and Stat5 (Supporting Information). Encouragingly, the potent EMSA  $IC_{50}$  value for **SF-1-066** was corroborated by a fluorescence polarization (FP) assay[25] ( $IC_{50} = 20 \mu\text{M}$ , Supporting Information). It is noteworthy that, whilst also corroborating the corresponding EMSA data ( $85 \mu\text{M}$ ), the FP-determined  $IC_{50}$  value for **S3I-201** was found to be  $80 \mu\text{M}$ , four times less potent than **SF-1-066**. It was anticipated that the FP-determined  $IC_{50}$  values would be more potent than their EMSA values because Stat3 is the only protein present in the former assay, whereas the analysis of nuclear extracts in the latter assay suggests the presence of several proteins, including the entire STAT family. These additional proteins might sequester the small molecule inhibitors from the assay medium, resulting in lower concentrations to bind the target protein Stat3, and, hence, apparently higher  $IC_{50}$  values.

When  $R^1 = (\textit{para}$ -cyclohexyl)benzyl, Stat3 inhibitory activity (as determined by EMSA analysis) was retained regardless of the X group: **SF-1-083**: X = NH,  $IC_{50} = 95 \mu\text{M}$ ; **SF-1-087** (Figure 2C): X = NBoc,  $IC_{50} = 115 \mu\text{M}$ ; **SF-1-121**: X = O,  $IC_{50} = 43 \mu\text{M}$  (Figure 2D). In all, these data show that *N*-alkylation of the amide bond with hydrophobic groups enhanced Stat3 inhibitory activity, and it is tempting to suggest that this finding is due to improved contacts between inhibitor and the Stat3 SH2 domain through the successful access of the third, hydrophobic subpocket (Trp623, Val637, Ile659 and Phe716). Indeed, a low-energy GOLD-docking solution of **SF-1-066** (Figure 3A) illustrates that, in addition to the salicylate and tosylamide moieties binding their predicted subpockets similarly to lead **S3I-201** (overlaid in Figure 3B), the (*para*-cyclohexyl)benzyl makes contacts with the third subpocket; this suggests that **SF-1-066** might be a more potent Stat3 inhibitor than **S3I-201**, and this has been found experimentally.

It is interesting to note that, within error, the affinities of the (*para*-cyclohexyl)benzyl derivatives **SF-1-121** (X = O:  $IC_{50} = 43 \mu\text{M}$  (EMSA),  $IC_{50} = 50 \mu\text{M}$  (FP)) and **SF-1-066** (X = NCH<sub>3</sub>:  $IC_{50} = 35 \mu\text{M}$  (EMSA),  $IC_{50} = 20 \mu\text{M}$  (FP)) for Stat3 are about the same, yet it is possible that the former might act as an irreversible inhibitor whilst the latter may not because it carries no leaving group. This is in stark contrast to the analogous compounds **S3I-201** and **SF-1-071** in which  $R^1 = \text{H}$  in both small molecules, and in which substituting X = O with X = NCH<sub>3</sub> led to a dramatic loss in inhibitor activity (**S3I-201** (X = O):  $IC_{50} = 86 \mu\text{M}$ ; **SF-1-071** (X = NCH<sub>3</sub>):  $IC_{50} > 300 \mu\text{M}$ ). It is therefore likely that the potent activity of **SF-1-121** is mostly derived from noncovalent interactions between inhibitor and the Stat3 SH2 domain, especially through the optimized  $R^1$  (*para*-cyclohexyl)-benzyl group (Figure 3).

Initial whole-cell activity of selected inhibitors (**SF-1-062**, **SF-1-066**, **SF-1-071**, **SF-1-087**, **SF-1-083** and **SF-1-084**), was investigated in v-Src-transformed mouse fibroblasts. Briefly, NIH3T3/v-Src cells were treated with inhibitors (at 100  $\mu$ M) for 48 h, and then the nuclear extracts were subjected to a Stat3–Stat3:DNA-binding assay in vitro by using the hSIE probe followed by EMSA analysis (Figure 4). Encouragingly, the potent Stat3 inhibitory activity of **SF-1-066** in vitro was reflected in this whole-cell assay, with **SF-1-066** completely inhibiting Stat3 dimerization at 100  $\mu$ M.

Further whole-cell activity of the most potent Stat3 agents was assessed in a range of human tumor cell lines known to contain constitutively activated Stat3 protein, including prostate cancer (DU145),[26] breast cancer (MDA468)[27a–c] and acute myeloid leukemia (OCI-AML-2)[28] cell lines (Table 2).[29] Significantly, several of our inhibitors represent potent antitumor agents with IC<sub>50</sub> values below 50  $\mu$ M for the three cancerous cell lines investigated (protocols outlined in the Supporting Information). Moreover, the WST-1 cell proliferation assay (Roche), used as a measure of inhibitor cytotoxicity, showed that **SF-1-066** exhibited concentration-dependent decreases in the viability of NIH3T3/v-Src and human pancreatic cancer Panc-1 cells, both of which harbor constitutively active Stat3 (Figure 5). Importantly, significant decreases in viability were observed at 30 and 50  $\mu$ M of **SF-1-066** as indicated by the drop in absorbance at 450 nm. In contrast, **SF-1-066** minimally affected normal mouse fibroblasts (NIH3T3), normal human pancreatic duct epithelial cells (HPDEC) and mouse fibroblasts overexpressing the human epidermal growth factor receptor (NIH3T3/hEGFR), none of which harbor persistent Stat3 activity (Figure 5). These data, in conjunction with the potent in vitro (Table 1) and whole-cell (Figure 4) results, suggest that **SF-1-066** is a Stat3-selective agent with a high specificity against tumor cells that exhibit constitutively activated Stat3.

In summary, we have developed a library of analogues of the previously reported Stat3 inhibitor **S3I-201**, the most potent member of which displays more than twice the original potency for Stat3 dimer disruption. Furthermore, the most active analogues **SF-1-066** and **SF-1-121** have shown impressive in vitro and whole-cell activities; this is possibly a result of the successful occupation of a third, hydrophobic subpocket of the Stat3 SH2 domain. In general, our studies demonstrate that appropriate scaffold extension into this subpocket, which is believed to be occupied by the R<sup>1</sup> substituent, resulted in significant increases in potency, thereby validating our approach to enhancing the Stat3 inhibitory activity of **S3I-201**. Future synthetic studies are currently focused upon developing extended agents with optimized occupation of the R<sup>1</sup> sub-pocket, as well as optimizing the sulfonamide portion of our inhibitors to enhance interactions in the tosylamide-binding subpocket.

## Supplementary Material

Refer to Web version on PubMed Central for supplementary material.

## Acknowledgments

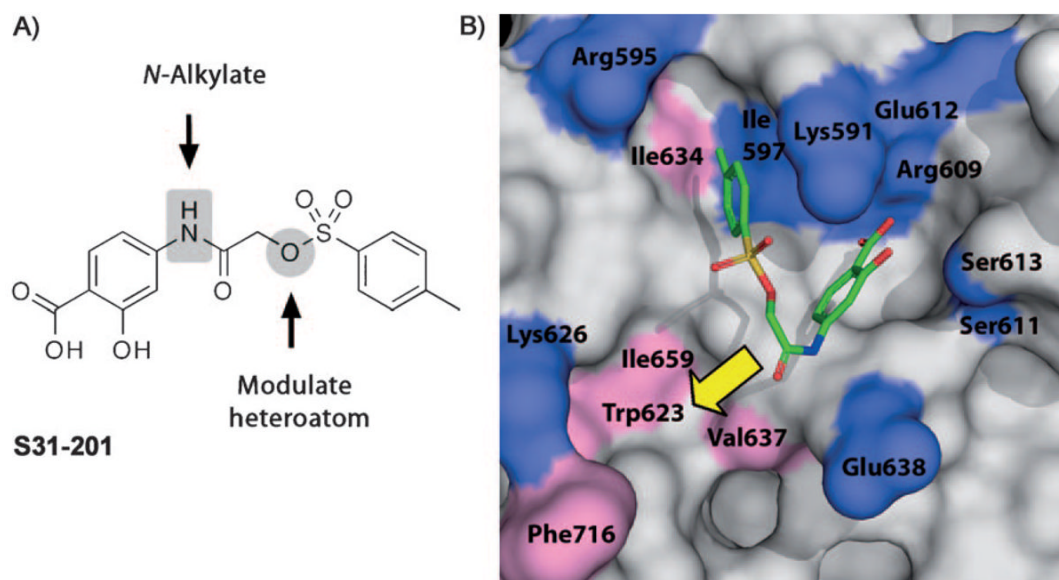
The authors would like to thank Jeffrey L. Wrana and Alessandro Datti (Mt. Sinai Hospital) for access to the SMART High-throughput screening facility. This work was supported by the Leukemia and Lymphoma Society of Canada (P.T.G.) and the University of Toronto (P.T.G.), and by the National Cancer Institute Grants CA106439 (J.T.) and CA128865 (J.T.). Aaron Schimmer is a Leukemia and Lymphoma Society Scholar in Clinical Research.

## References

1. a) Fletcher S, Turkson J, Gunning PT. *ChemMedChem* 2008;3:1159–1168. [PubMed: 18683176] b) Burke WM, Jin X, Lin HJ, Huang M, Liu R, Reynolds KR, Lin J. *Oncogene* 2001;20:7925–7934. [PubMed: 11753675] c) Berishaj M, Gao SP, Leslie K, Al-Ahmadie H, Gerald WL, Bornmann W,

- Bromberg JF. *Breast Cancer Res* 2007;3:1–8. d) Berg T. *ChemBioChem* 2008;9:2039–2044. [PubMed: 18677740] e) Peibin Y, Turkson J. *Expert Opin Invest Drugs* 2009;18:45–56.
2. a) Darnell JE Jr. *Recent Prog Horm Res* 1996;51:391–403. [PubMed: 8701087] b) Darnell JE Jr. *Science* 1997;277:1630–1635. [PubMed: 9287210]
  3. Turkson J, Ryan D, Kim JS, Zhang Y, Chen Z, Haura E, Laudano A, Sebti SM, Hamilton AD, Jove R. *J Biol Chem* 2001;276:45443–45455. [PubMed: 11579100]
  4. Ren Z, Cabell LA, Schaefer TS, McMurray JS. *Bioorg Med Chem Lett* 2003;13:633–636. [PubMed: 12639546]
  5. Gunning PT, Katt WP, Glenn MP, Siddiquee KAZ, Kim JS, Jove R, Sebti SM, Turkson J, Hamilton AD. *Bioorg Med Chem Lett* 2007;17:1875–1878. [PubMed: 17336521]
  6. Coleman DR IV, Ren R, Mandal PK, Cameron AG, Dyer GA, Muranjan S, Chen X, McMurray JS. *J Med Chem* 2005;48:6661–6670. [PubMed: 16220982]
  7. Mandal PK, Heard PA, Ren Z, Chen X, McMurray JS. *Bioorg Med Chem Lett* 2007;17:654–656. [PubMed: 17113289]
  8. Chen J, Nikolovska-Coleska Z, Yang CY, Gomez C, Gao W, Krajewski K, Jiang S, Roller P, Wang S. *Bioorg Med Chem Lett* 2007;17:3939–3942. [PubMed: 17513110]
  9. Dourlat J, Valentin B, Liu WC, Garbay C. *Bioorg Med Chem Lett* 2007;17:3939–3942. [PubMed: 17513110]
  10. Gunning PT, Glenn M, Siddiquee KAZ, Katt WP, Masson E, Sebti SM, Turkson J, Hamilton AD. *ChemBioChem* 2008;9:2800–2803. [PubMed: 19006150]
  11. Siddiquee K, Gunning PT, Glenn M, Glenn WP, Sebti SM, Jove R, Hamilton AD, Turkson J. *ACS Chem Biol* 2007;2:787–796. [PubMed: 18154266]
  12. Siddiquee K, Zhang S, Guida WC, Blaskovich MA, Greedy B, Lawrence HR, Yip MLR, Jove R, Laughlin MM, Lawrence NJ, Sebti SM, Turkson J. *Proc Natl Acad Sci USA* 2007;104:7391–7396. [PubMed: 17463090]
  13. Schust J, Sperl B, Hollis A, Mayer TU, Berg T. *Chem Biol* 2006;13:1235–1242. [PubMed: 17114005]
  14. Song H, Wang R, Wang S, Lin J. *Proc Natl Acad Sci USA* 2005;102:4700–4705. [PubMed: 15781862]
  15. Turkson J, Zhang S, Palmer J, Kay H, Stanko J, Mora LB, Sebti S, Yu H, Jove R. *Mol Cancer Ther* 2004;3:1533–1542. [PubMed: 15634646]
  16. a) Fletcher S, Hamilton AD. *J R Soc Interface* 2006;3:215–233. [PubMed: 16849232] b) Fletcher S, Hamilton AD. *Curr Opin Chem Biol* 2005;9:632–638. [PubMed: 16242379] c) Fletcher S, Hamilton AD. *Curr Top Med Chem* 2007;7:922–927. [PubMed: 17508923]
  17. a) Buettner R, Mora LB, Jove R. *Clin Cancer Res* 2002;8:945–954. [PubMed: 11948098] b) Darnell JE Jr. *Nat Med* 2005;11:595–596. [PubMed: 15937466] c) Bowman T, Garcia R, Turkson J, Jove R. *Oncogene* 2000;19:2474–2488. [PubMed: 10851046]
  18. Jones G, Willett P, Glen RC, Leach AC, Taylor R. *J Mol Biol* 1997;267:727. [PubMed: 9126849]
  19. Becker S, Groner B, Muller CW. *Nature* 1998;394:145–151. [PubMed: 9671298]
  20. Zhang S, Zhang ZY. *Drug Discovery Today* 2007;12:373–381. [PubMed: 17467573]
  21. Maegawa T, Fujita Y, Sakurai A, Akashi A, Sato M, Oono K, Sajiki H. *Chem Pharm Bull* 2007;55:837–839. [PubMed: 17473483]
  22. Pandey PN, Purkayastha ML. *Synthesis* 1982:876–878. and references therein.
  23. Fletcher S, Gunning PT. *Tetrahedron Lett* 2008;49:4817–4819.
  24. Zhang X, Yue P, Fletcher S, Zhao W, Gunning PT, Turkson J. *J Biol Chem*. 2009 submitted.
  25. Schust J, Berg T. *Anal Biochem* 2004;330:114–118. [PubMed: 15183768]
  26. Alimirah F, Chen J, Basrawala Z, Xin H, Choubey D. *FEBS Lett* 2006;580:2294–2300. [PubMed: 16580667]
  27. a) Filmus J, Trent JM, Pollak MN, Buick RN. *Mol Cell Biol* 1987;7:251–257. [PubMed: 3494191] b) Garcia R, Bowman TL, Nui G, Yu H, Minton S, Muro-Cacho CA, Cox CE, Falcone R, Fairclough R, Parsons S, Laudano A, Gazit A, Levitzki A, Kraker A, Jove R. *Oncogene* 2001;20:2499–2513. [PubMed: 11420660] c) Mora LB, Buettner R, Seigne J, Diaz J, Ahmad N,

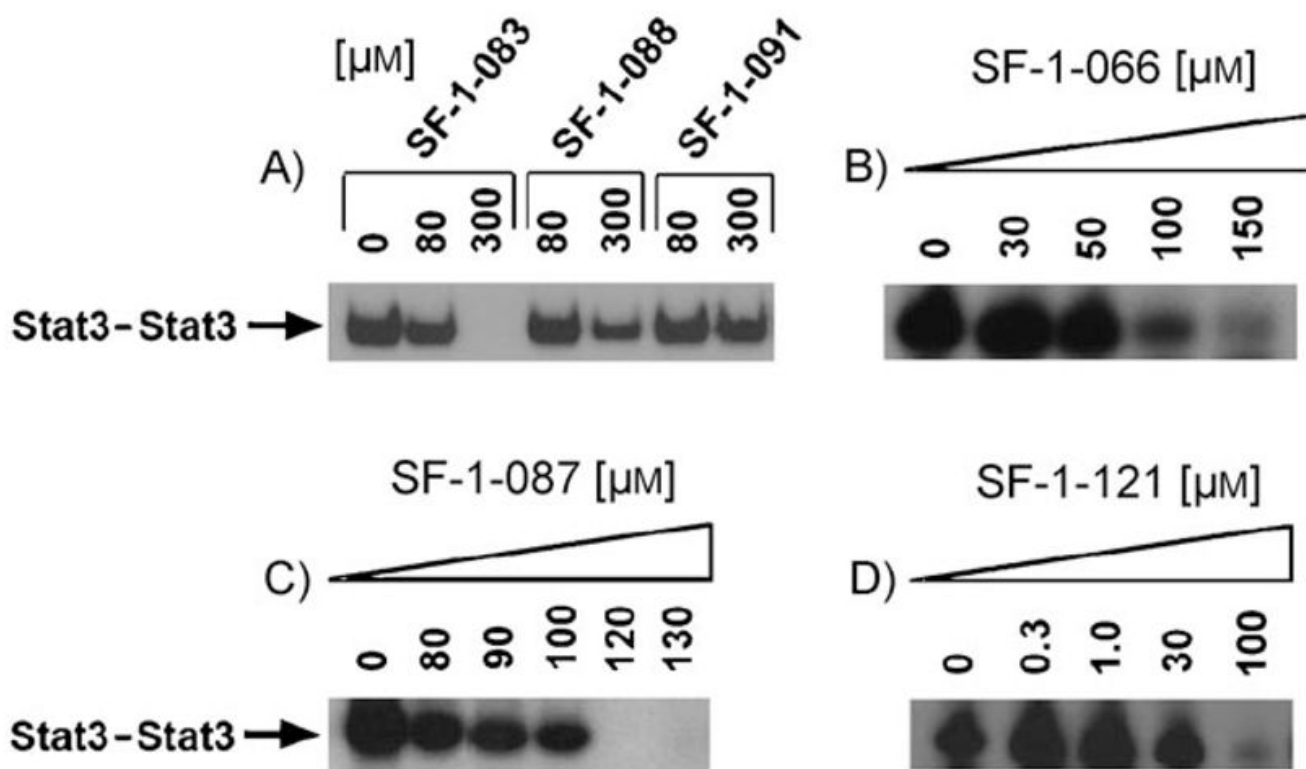
- Garcia R, Bowman T, Falcone R, Fairclough R, Cantor A, Muro-Cacho C, Livingston S, Karras J, Pow-Sang J, Jove R. *Cancer Res* 2002;62:6659–6666. [PubMed: 12438264]
28. Wang C, Curtis JE, Minden MD, McCulloch EA. *Leukemia* 1989;3:264–269. [PubMed: 2538684]
29. Simpson CD, Mawji IA, Anyiwe K, Williams MA, Wang X, Venugopal AL, Gronda M, Hurren R, Cheng S, Serra S, Zavareh RB, Datti A, Wrana JL, Ezzat S, Schimmer AD. *Cancer Res* 2009;69:2739–2749. [PubMed: 19293189]



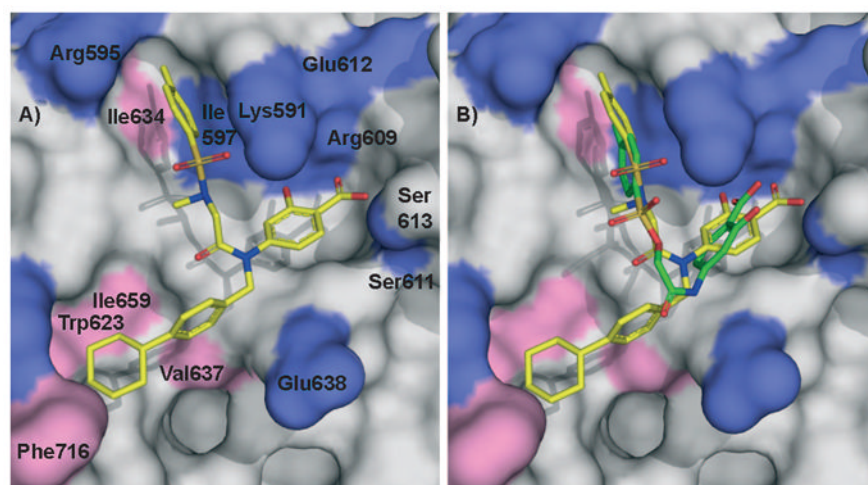
**Figure 1.**

A) Proposed synthetic modification to **S3I-201**. B) Low-energy GOLD[18]-docked **S3I-201** (green) in the Stat3 SH2 domain (PDB ID: 1BG1): pink = hydrophobic residues, blue = hydrophilic residues.[19] Arrow denotes potential binding pocket.

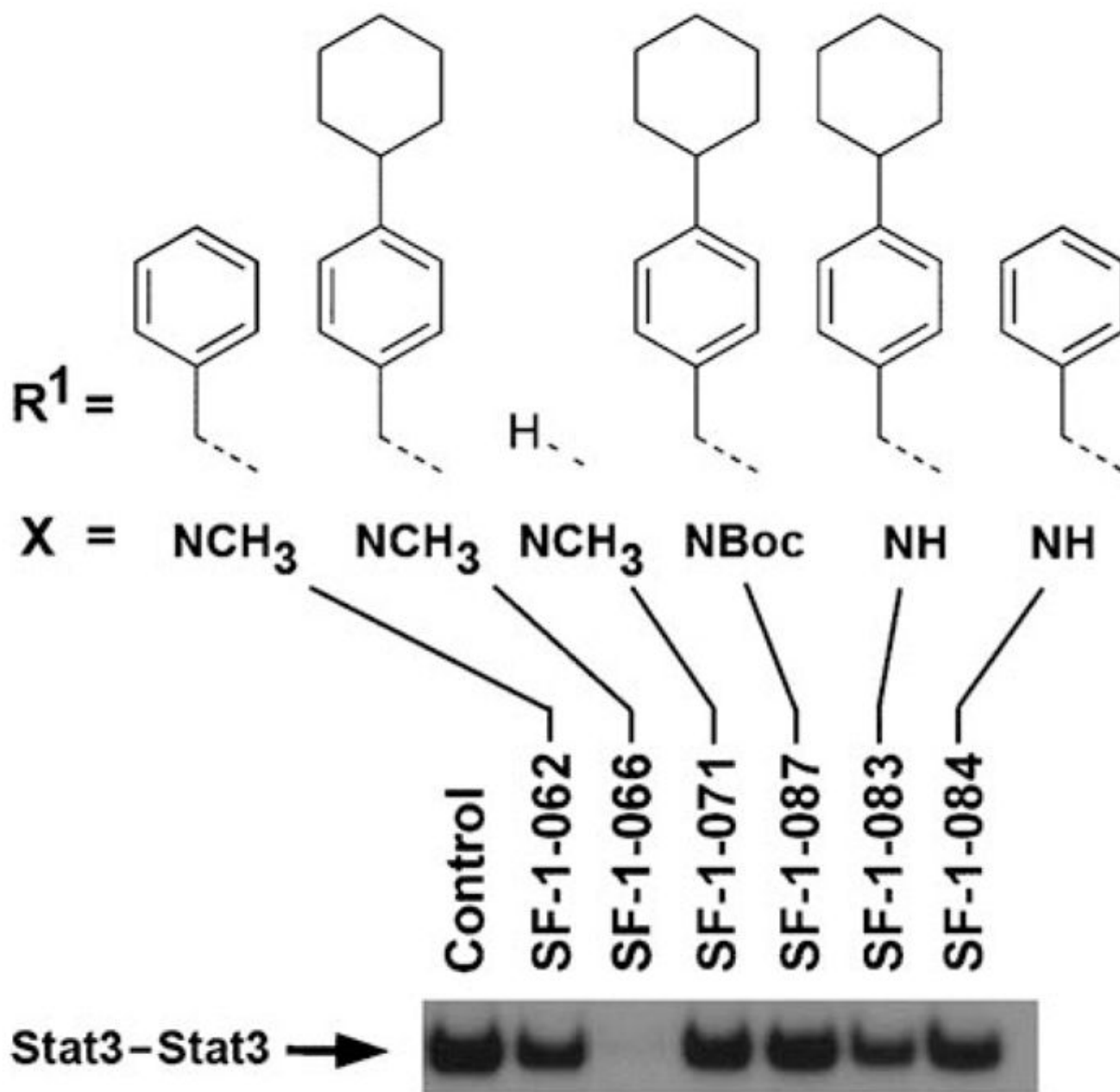




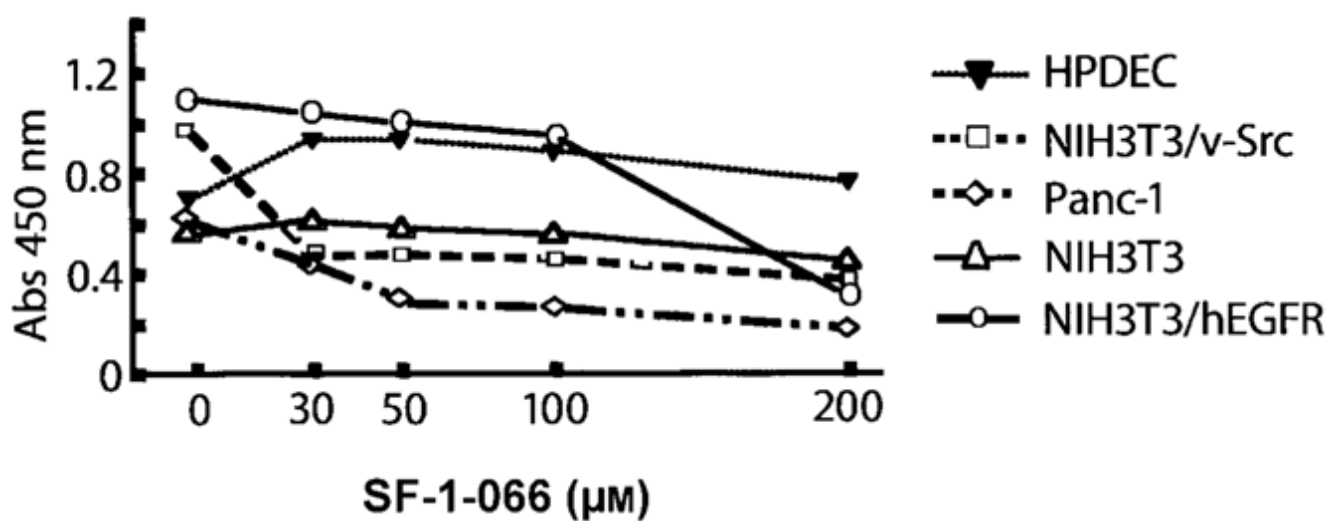
**Figure 2.** Electrophoretic mobility shift assay (EMSA) analyses of Stat3-Stat3 dimerization inhibition (as judged by the disruption of the Stat3-Stat3:DNA complex) with small molecule agents. Nuclear extracts containing activated Stat3 were pretreated with the indicated concentrations of inhibitors (A) **SF-1-083**, **SF-1-088**, **SF-1-091**; B) **SF-1-066**; C) **SF-1-087**; D) **SF-1-121**) prior to incubation with the radiolabeled high-affinity sis-inducible element (hSIE) probe that binds Stat3, and then subjected to EMSA analysis. Positions of Stat3-Stat3:DNA complexes in gel are shown; data are representative of three independent assays.



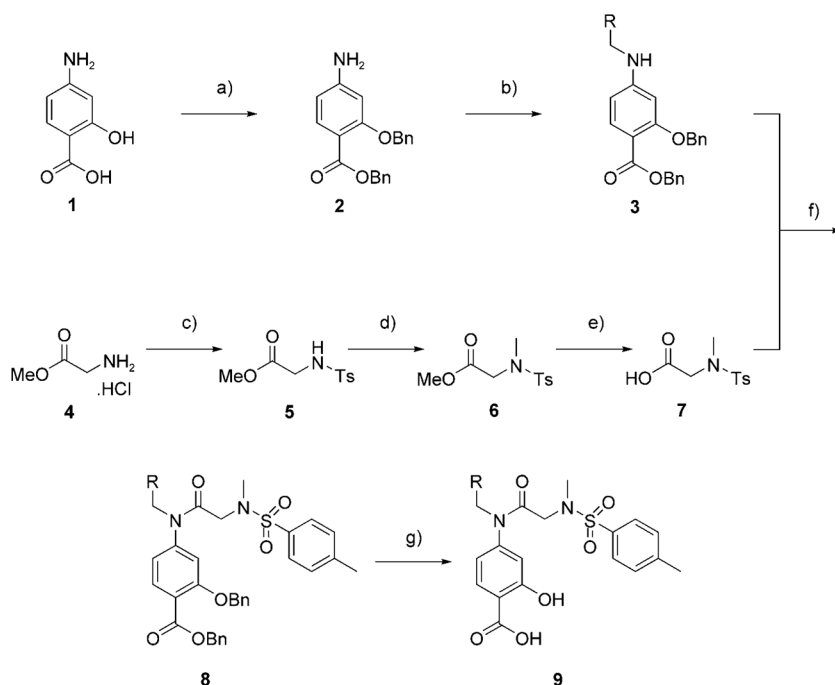
**Figure 3.**  
A) Low-energy GOLD-docked **SF-1-066** (yellow) in the Stat3 $\beta$  homodimer (PDB ID: 1BG1). B) Comparative GOLD docking of **S3I-201** (green) and **SF-1-066** (yellow) within the SH2 domain of Stat3 protein: pink = hydrophobic residues, blue = hydrophilic residues.



**Figure 4.** EMSA analyses of whole-cell (NIH3T3/v-Src) Stat3-Stat3 dimerization inhibition (as judged by the disruption of the Stat3-Stat3:DNA complex) with selected small molecule agents at 100  $\mu$ M (control = small molecule inhibitor absent), as described previously.[3] Positions of Stat3-Stat3:DNA complexes in gel are shown; data are representative of two independent assays.



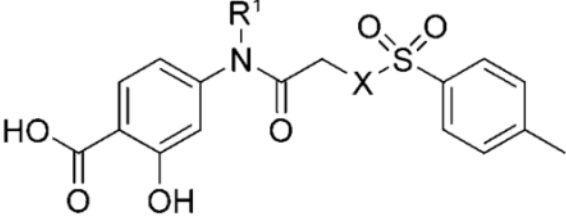
**Figure 5.** WST-1 viability assay for effects of **SF-1-066** on normal and malignant cells in culture. Cells growing in culture in 96-well plates were treated with increasing concentrations of **SF-1-066** for 48 h, processed for WST-1 assay (Roche), and absorbances of samples in wells were determined at 450 nm.

**Scheme 1.**

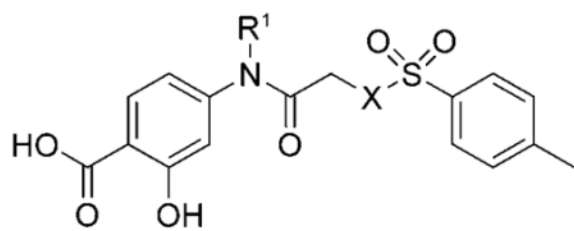
a) 1. BnBr, KO $t$ Bu, DMF, 0 °C $\rightarrow$ RT, 5 h; 2. BnBr, KO $t$ Bu, DMF, 0 °C $\rightarrow$ RT, 16 h, 54 %; b) 1. RCHO, AcOH, 4 & MS, MeOH, 45 °C, 3 h; 2. NaCNBH $_3$ , RT, 12 h, 75–96 %; c) *p*-TsCl, *i*Pr $_2$ EtN, CH $_3$ CN, 0 °C $\rightarrow$ RT, 1 h, 93 %; d) MeI, Cs $_2$ CO $_3$ , DMF, RT, 16 h, 85 %; e) LiOH $\cdot$ H $_2$ O, THF/MeOH/H $_2$ O (3:1:1), RT, 1 h, 95 %; f) PPh $_3$ Cl $_2$ , CHCl $_3$ , 60 °C, 12 h, 89–95 %; g) H $_2$ , 10 % Pd/C, MeOH/THF, 1:1, RT, 1–16 h, 85–100%. *p*-TsCl = *para*-toluenesulfonyl chloride; DMF = *N,N*-dimethylformamide; THF = tetrahydrofuran.

**Table 1**

Table of in vitro Stat3–Stat3:DNA disruption IC<sub>50</sub> data (EMSA) for **S3I-201** analogue inhibitors. Structural modifications (R<sup>1</sup> and X) are out-lined.



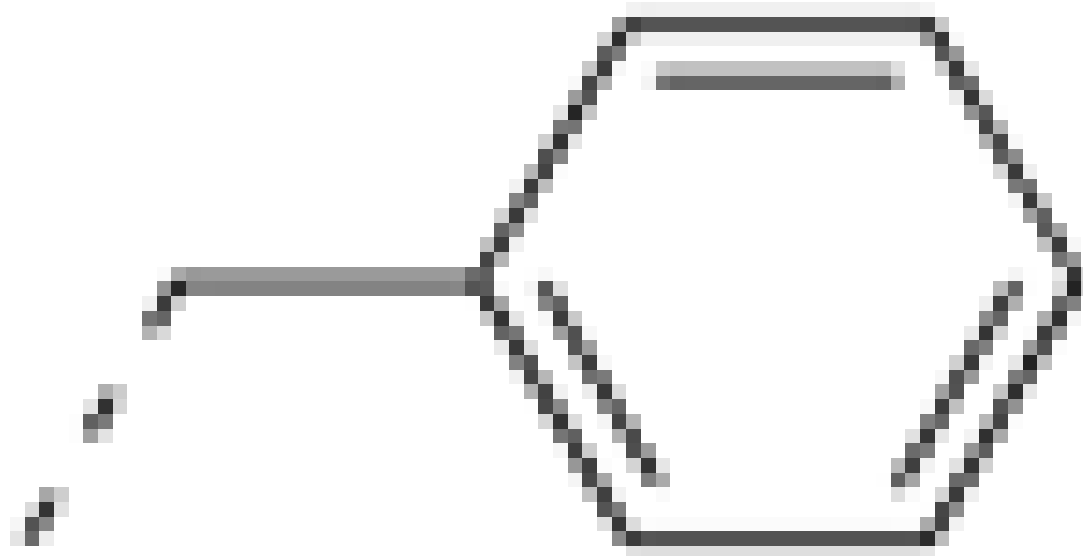
Inhibitor	R <sup>1</sup>	X
<b>S3I-201</b>	H	O
<b>SF-1-082</b>	H	NH
<b>SF-1-071</b>	H	NCH <sub>3</sub>
<b>SF-1-091</b>	H	NBoc
<b>SF-1-086</b>	Boc	NBoc
<b>SF-1-120</b>		O

Inhibitor R<sup>1</sup>

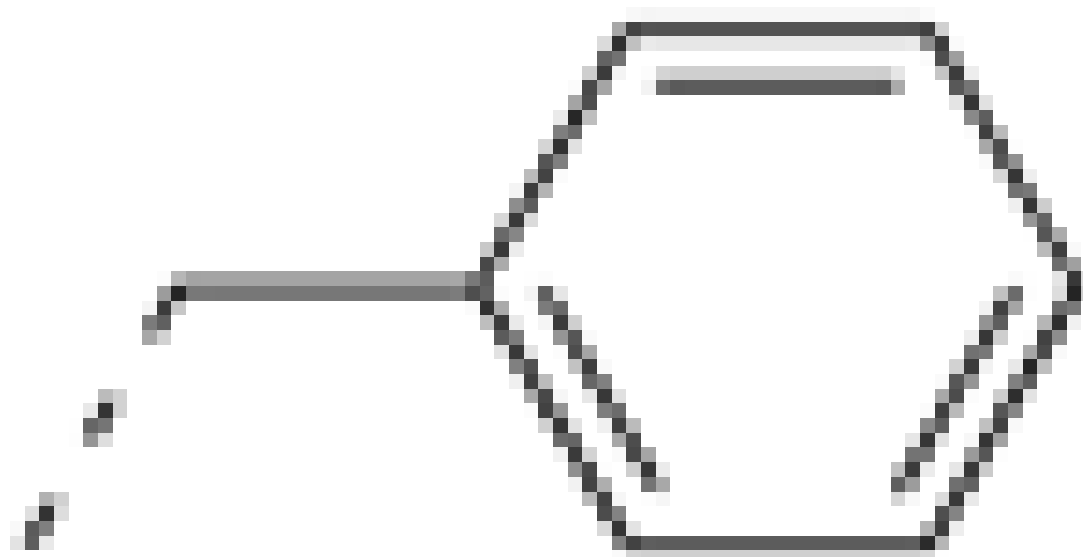
X

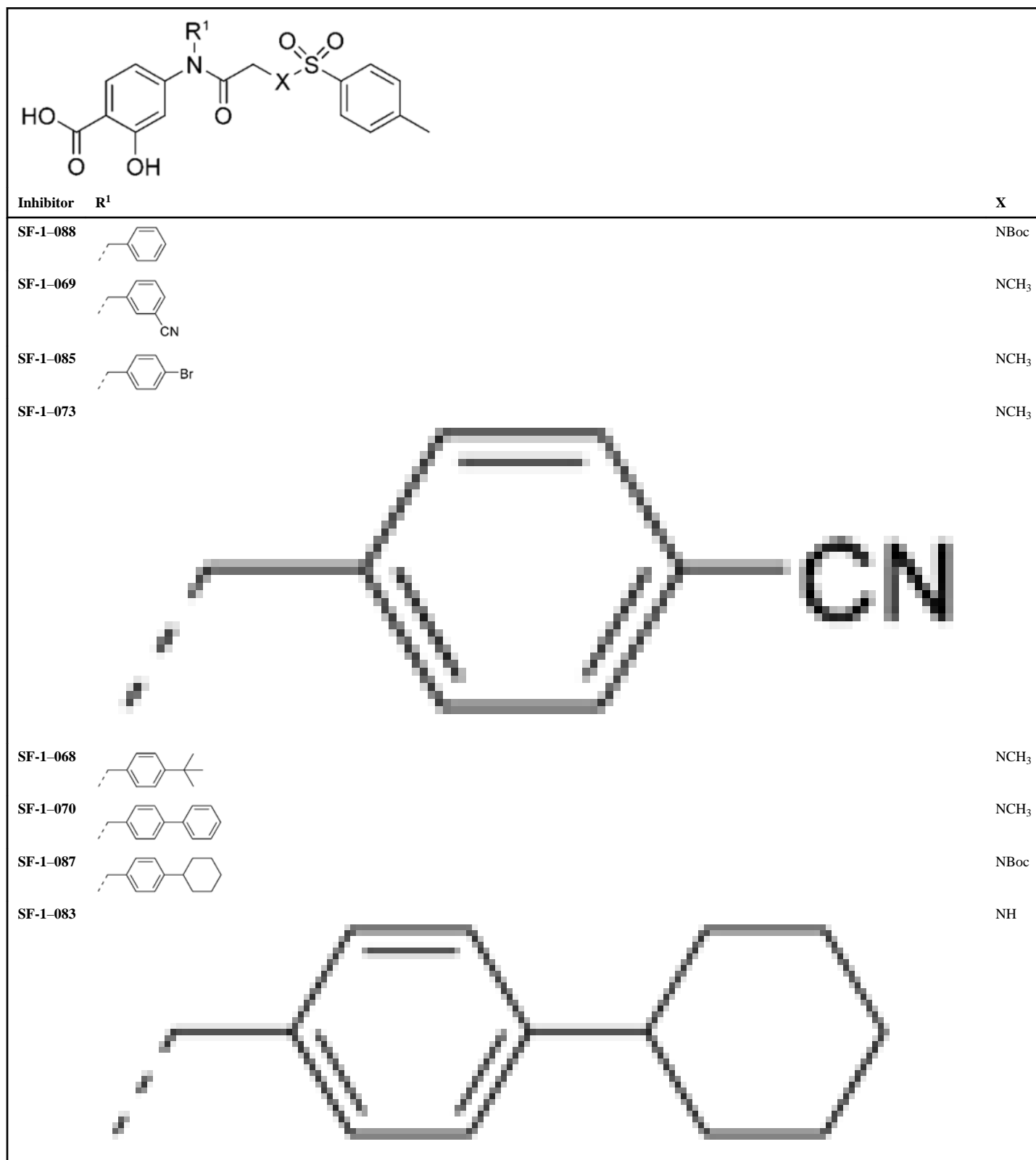
SF-1-084

NH



SF-1-062

NCH<sub>3</sub>





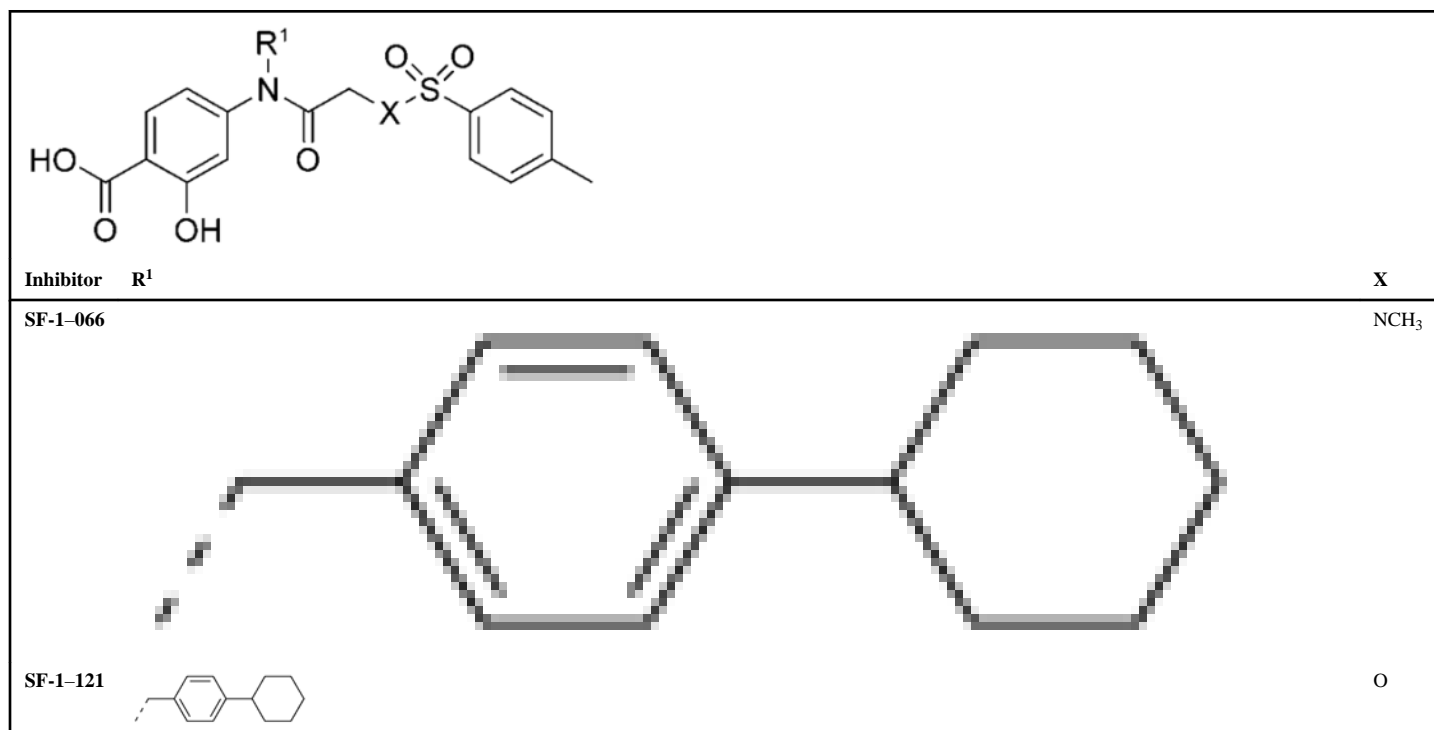


**Table 2**

IC<sub>50</sub> values [ $\mu$ M] for selected inhibitors in whole-cell viability studies in DU145<sup>[a]</sup> MDA468<sup>[b]</sup> and OCI-AML-2<sup>[c]</sup> cell lines.

Inhibitor	DU145	MDA468	OCI-AML-2
<b>S3I-201</b>	75 $\pm$ 9.4	27.9 $\pm$ 2.9	112 $\pm$ 10.1
<b>SF-1-068</b>	63.7 $\pm$ 4.5	34.9 $\pm$ 9.4	68.3 $\pm$ 1.2
<b>SF-1-121</b>	51.9 $\pm$ 12.9	42.6 $\pm$ 5.8	62.0 $\pm$ 12.3
<b>SF-1-083</b>	38.4 $\pm$ 14.4	21.4 $\pm$ 6.2	33.0 $\pm$ 7.7
<b>SF-1-066</b>	37.2 $\pm$ 12.4	17.0 $\pm$ 4.4	35.9 $\pm$ 13.1
<b>SF-1-087</b>	24.5 $\pm$ 15.9	10.5 $\pm$ 9.4	18.0 $\pm$ 8.9

[a] Prostate cancer.

[b] Breast cancer.

[c] Acute myeloid leukemia.